

Accelerated ADMM: Automated Parameter Tuning and Improved Linear Convergence

M. Tavakoli ^{*,†} F. Jakob ^{**,†} G. Carnevale ^{*} G. Notarstefano ^{*}
A. Iannelli ^{**}

^{*} Università di Bologna, Department of Electrical, Electronic and Information Engineering, Bologna, Italy (e-mail: meisam.tavakoli@studio.unibo.it, guido.carnevale, giuseppe.notarstefano@unibo.it).

^{**} University of Stuttgart, Institute for Systems Theory and Automatic Control, Stuttgart, Germany (e-mail: fabian.jakob, andrea.iannelli@ist.uni-stuttgart.de).

[†] The first two authors contributed equally to this work.

Abstract: This work studies the linear convergence of an accelerated scheme of the Alternating Direction Method of Multipliers (ADMM) for strongly convex and Lipschitz-smooth problems. We use the methodology of expressing the accelerated ADMM as a Lur'e system, i.e., an interconnection of a linear dynamical system in feedback with a slope-restricted operator, and we use Integral Quadratic Constraints to establish linear convergence. In addition, we propose several parameter tuning heuristics and their impact on the convergence rate through numerical analyses. Our new bounds show significantly improved linear convergence rates compared to the vanilla algorithm and previous proposed accelerated variants, which is also empirically validated on a LASSO regression benchmark.

Keywords: ADMM, First-order optimization, Lur'e systems, Integral Quadratic Constraints

1. INTRODUCTION

The Alternating Direction Method of Multipliers (ADMM) (Glowinski and Marroco, 1975; Boyd et al., 2011) has emerged as a benchmark algorithm among first-order methods for solving convex composite optimization problems. Its ability to decompose the original problem into subproblems that can be solved in parallel made it especially popular in computation-heavy domains as signal processing, machine learning or distributed control.

It is long established that ADMM enjoys provable convergence guarantees in the convex setting. In particular, Deng and Yin (2016) showed that for general convex problems ADMM achieves $\mathcal{O}(1/k)$ convergence rate, while for the strongly convex and smooth case it attains a linear convergence rate. An alternative proof of linear convergence was provided by Nishihara et al. (2015), who applied the Integral Quadratic Constraints (IQC) framework (Megretski and Rantzer, 1997; Lessard et al., 2016; Michalowsky et al., 2021) to numerically derive convergence rates and heuristics for parameter tuning. The proof frames the optimization algorithm as a Lur'e system (a feedback interconnection of an LTI system and monotone operators), and casts the convergence analysis as a stability problem. This framework offers the main advantage that also the analysis of altered schemes, such as over-relaxed variants,

can be seamlessly carried out in an automated fashion as long as they can be framed in the Lur'e setting.

Also accelerated variants of ADMM (A-ADMM) have been proposed and analyzed in recent years. Goldstein et al. (2014) showed that Nesterov acceleration leads to a convergence rate of $\mathcal{O}(1/k^2)$ in the strongly convex settings. Wang et al. (2021) provided linear convergence guarantees when Anderson acceleration is applied. Patrinos et al. (2014); Pejcic and Jones (2016) proved linear convergence of accelerated Douglas–Rachford splitting and ADMM for strongly convex quadratic problems, showing that the optimal rate matches that of Nesterov's fast gradient method. However, an analysis of the convergence rates of A-ADMM for general strongly convex and smooth problems is still unaddressed, as well as the question of whether other known rates from classical accelerated gradient methods can be matched.

In this work, we extend the IQC-based analysis of vanilla ADMM (Nishihara et al., 2015) to the accelerated case, when one of the objectives is strongly convex and smooth. By casting the A-ADMM algorithm as a Lur'e system, we propose a semi-definite program (SDP) that provides a numerical tool to theoretically verify worst-case convergence rates of accelerated schemes. Using dynamic O'Shea-Zames-Falb (OZF) IQCs (Boczar et al., 2015), we prove that A-ADMM achieves tighter worst-case convergence bounds than vanilla ADMM. Moreover, we propose a systematic parameter tuning procedure

¹ F. Jakob acknowledges the support of the International Max Planck Research School for Intelligent Systems (IMPRS-IS).

Table 1. Contextualization of the results. Here, $\rho_1 = 1 - \frac{1}{\sqrt{\kappa}}$ and $\rho_2 = \sqrt{1 - \frac{\sqrt{2\kappa-1}}{\kappa}}$ with $\kappa = \frac{L}{m}$. NM and TM stand for Nesterov and Triple Momentum parameter selections (see Table 2).

Setting	Objective f	Algorithm	Rate ρ	Reference
$\min f(x)$	Quadr.	Nesterov Method	ρ_1	Nesterov (2004)
$\min f(x)$	$S(m, L)$	Nesterov Method	ρ_2	Safavi et al. (2018)
$\min f(x)$	$S(m, L)$	Triple Momentum	ρ_1	Van Scy et al. (2018)
(1)	Quadr.	A-ADMM (NM)	ρ_1	Patrinos et al. (2014); Pejcic and Jones (2016)
(1)	$S(m, L)$	A-ADMM (NM)	Fig. 1a	This work
(1)	$S(m, L)$	A-ADMM (TM)	Fig. 1b	This work

based on this framework and demonstrate that Nesterov- and Triple-Momentum-inspired parameter selections attain rates close to those of accelerated first-order methods (cf. Table 1). Finally, we identify through grid search a new A-ADMM configuration with the fastest certified convergence rate, which also exhibits the best empirical performance in our numerical experiments. Our theoretical results are validated on a LASSO regression case study, showing improved convergence speed of all our schemes compared to existing benchmark algorithms.

The remainder of the paper is organized as follows. Section 2 presents the problem setup, the ADMM formulation, and the required IQC preliminaries. Section 3 provides a Lur'e representation of the A-ADMM scheme. In Section 4, we study the convergence rates of this A-ADMM scheme under different parameter configurations. In Section 5, we provide a case study on LASSO regression. Finally, Section 6 concludes the paper.

Notation. The identity matrix of dimension p is denoted as I_p . The gradient and subdifferential of a function f are denoted by ∇f and ∂f , respectively. For $0 < m \leq L < \infty$, we let $S_p(m, L)$ denote the class functions $f : \mathbb{R}^p \rightarrow \mathbb{R}$ that are m -strongly convex and have L -Lipschitz continuous gradients. The special case $S_p(0, \infty)$ corresponds to the set of proper, closed and convex functions. For a matrix M , its condition number is defined as $\kappa_M = \bar{\sigma}(M)/\underline{\sigma}(M)$, where $\bar{\sigma}(M)$ and $\underline{\sigma}(M)$ denote the largest and smallest singular values of M , respectively. A discrete-time LTI system maps the signals $u \mapsto y$ via the recursion $\xi_{k+1} = A\xi_k + Bu_k$, $y_k = C\xi_k + Du_k$ as an ξ_0 dependent mapping, and will be compactly expressed as $y = Gu$ with $G = \begin{bmatrix} A & B \\ C & D \end{bmatrix}$.

We write $G \otimes I_d$ to define a lifted system $\begin{bmatrix} A \otimes I_d & B \otimes I_d \\ C \otimes I_d & D \otimes I_d \end{bmatrix}$. The series interconnection between two LTI systems $G_1 : u \mapsto y$ and $G_2 : y \mapsto w$ will be denoted as $G_1 \cdot G_2 : u \mapsto w$. The forward shift operator is denoted as \mathbf{z} .

2. PRELIMINARIES

2.1 Accelerated ADMM

We consider constrained convex optimization problems of the form

$$\min_{x \in \mathbb{R}^p, z \in \mathbb{R}^q} f(x) + g(z) \quad \text{s.t.} \quad Ax + Bz = c, \quad (1)$$

where $f : \mathbb{R}^p \rightarrow \mathbb{R}$, $f \in S_p(m, L)$ and $g : \mathbb{R}^q \rightarrow \mathbb{R}$, $g \in S_q(0, \infty)$. The matrices $A \in \mathbb{R}^{p \times p}$, $B \in \mathbb{R}^{p \times q}$, and $c \in \mathbb{R}^p$ define linear equality constraints coupling the variables x and z , where we particularly assume that A is invertible and that B has full column rank. Having a

strongly convex and smooth component in (1) is common in many practical applications (Deng and Yin, 2016), while restricting A to be square and invertible is slightly restrictive, but also done in Nishihara et al. (2015). We note that still many practical problem instances satisfy this structure, including consensus problems and various distributed optimization tasks (Notarstefano et al., 2019).

To address problem (1), we use the over-relaxed ADMM algorithm (Boyd et al., 2011)

$$x_{k+1} = \arg \min_x f(x) + \frac{1}{2\nu_1} \|Ax + B\hat{z}_k - c + \hat{\lambda}_k\|^2 \quad (2a)$$

$$z_{k+1} = \arg \min_z g(z) + \frac{1}{2\nu_1} \|\alpha Ax_{k+1} - (1 - \alpha)Bz_k + Bz - \alpha c + \hat{\lambda}_k\|^2 \quad (2b)$$

$$\lambda_{k+1} = \alpha Ax_{k+1} - (1 - \alpha)Bz_k + Bz_{k+1} - \alpha c + \hat{\lambda}_k \quad (2c)$$

as starting point, and augment it with a *momentum-term*

$$\hat{z}_k = z_k + \nu_2(z_k - z_{k-1}) \quad (3a)$$

$$\hat{\lambda}_k = \lambda_k + \nu_2(\lambda_k - \lambda_{k-1}), \quad (3b)$$

as in Goldstein et al. (2014); Pejcic and Jones (2016). Here, $\nu_1 > 0$ is a step size, $\nu_2 \geq 0$ a momentum parameter and $\alpha \geq 0$ the so-called over-relaxation parameter. We recover the nominal A-ADMM by setting $\alpha = 1$, and the vanilla, non-accelerated ADMM with $\nu_2 = 0$. Both α and ν_2 have been shown to improve the convergence speed for suitable choices (Eckstein and Bertsekas, 1992; Patrinos et al., 2014). The over-relaxation parameter α is chosen in the interval $(0, 2]$, while ν_2 is often selected according to Nesterov's schemes (Nesterov, 2004), e.g., $\nu_2 = (\sqrt{L} - \sqrt{m})/(\sqrt{L} + \sqrt{m})$ (Patrinos et al., 2014), or as an iteration dependent quantity (Goldstein et al., 2014). To explore alternative parameter selection strategies we employ the IQC framework.

2.2 Integral Quadratic Constraints for Convex Functions

Algorithm (2)-(3) will be analyzed as a dynamical system converging to points satisfying the first-order optimality conditions. We will make use of the well-known fact that (sub)gradients of (strongly) convex functions are monotone and, thus, their input/output relation satisfy IQCs for slope-restricted operators (Lessard et al., 2016). To be more precise, they have been shown to fulfill so-called ρ -hard O'Shea-Zames-Falb IQCs.

Proposition 1. (ρ -OZF IQC, Boczar et al. (2015)). Let $f \in S_p(m, L)$, $g \in S_q(0, \infty)$ and let $\rho \in (0, 1)$ be an exponential discount factor. For $n_{\text{OZF}} \in \mathbb{N}_0$, let $\{h_\tau^f\}_{\tau=0}^{n_{\text{OZF}}}$ and $\{h_\tau^g\}_{\tau=0}^{n_{\text{OZF}}}$ be sequences of filter coefficients satisfying

$$h_\tau^* \leq 0 \quad \forall \tau \neq 0, \quad \sum_{\tau=0}^{n_{\text{OZF}}} \rho^{-2\tau} h_\tau^* \geq 0, \quad * \in \{f, g\} \quad (4)$$

and define the parametrized LTI filters

$$\Psi_g(h^g) = \begin{bmatrix} \sum_{\tau=0}^{n_{\text{OZF}}} h_\tau^g \mathbf{z}^{-\tau} & 0 \\ 0 & 1 \end{bmatrix}, \quad \Psi_f(h^f) = \Psi_g(h^f) \cdot \begin{bmatrix} L & -1 \\ -m & 1 \end{bmatrix}. \quad (5)$$

Let $\{a_k\}, \{b_k\}$ be some p -dim. square summable sequences and let $a^*, b^* \in \mathbb{R}^p$ be constant references. For $\gamma_k \in \partial g(b_k)$ and $\gamma^* \in \partial g(b^*)$, define

$$\begin{aligned} \tilde{a}_k &= a_k - a^*, & \nabla \tilde{f}_k &= \nabla f(a_k) - \nabla f(a^*), \\ \tilde{b}_k &= b_k - b^*, & \tilde{\gamma}_k &= \gamma_k - \gamma^*. \end{aligned}$$

Finally, define the filtered sequences

$$\psi_{1,k} = (\Psi_f \otimes I_p) \begin{bmatrix} \tilde{a}_k \\ \nabla \tilde{f}_k \end{bmatrix}, \quad \psi_{2,k} = (\Psi_g \otimes I_p) \begin{bmatrix} \tilde{b}_k \\ \tilde{\gamma}_k \end{bmatrix}$$

and $M = \begin{bmatrix} 0 & 1 \\ 1 & 0 \end{bmatrix}$. Then, for all $T \geq 0$, it holds

$$\sum_{k=0}^T \rho^{-2k} \psi_{i,k}^\top (M \otimes I_p) \psi_{i,k} \geq 0, \quad i = 1, 2. \quad (6)$$

The filter coefficients h^f, h^g will serve as degree-of-freedom in the resulting SDP, subject to the convex constraint (4). In theory, the filter dimension n_{OZF} can be infinite, but is chosen finite in practice to yield finite-dimensional state-space realizations. A choice of $n_{\text{OZF}} = 0$ leads to static filters Ψ_f, Ψ_g and pointwise satisfaction of the inequalities (6), which in literature is often referred to as sector IQC (Lessard et al., 2016).

2.3 Stability Analysis of First-Order Algorithms

Consider the following Lur'e representation of a first-order algorithm

$$\begin{aligned} \xi_{k+1} &= (\hat{A} \otimes I_p) \xi_k + (\hat{B} \otimes I_p) w_k \\ \hat{v}_k &= (\hat{C} \otimes I_p) \xi_k + (\hat{D} \otimes I_p) w_k \end{aligned} \quad (7a)$$

with state $\xi_k \in \mathbb{R}^{n_\xi}$, output $\hat{v}_k = v_k + \bar{v}$ for some constant offset \bar{v} , and

$$v_k = \begin{bmatrix} v_{1,k} \\ v_{2,k} \end{bmatrix}, \quad w_k = \begin{bmatrix} \nabla \hat{f}(v_{1,k}) \\ \gamma_k \end{bmatrix}, \quad \gamma_k \in \partial \hat{g}(v_{2,k}), \quad (7b)$$

where $\hat{f} \in S_p(\hat{m}, \hat{L})$, $\hat{g} \in S_p(0, \infty)$ for some \hat{m}, \hat{L} . It has been shown that ADMM, but also many other first-order algorithms, can be represented as (7) (Nishihara et al., 2015) when \hat{f}, \hat{g} are suitably chosen. In general, $(\hat{A}, \hat{B}, \hat{C}, \hat{D})$ fulfill structural assumptions such that its fixed-point (ξ^*, \hat{v}^*, w^*) is unique and satisfies first-order optimality (Upadhyaya et al., 2024). Showing exponential stability of (7) is therefore the same as showing linear convergence of the underlying algorithm. With a coordinate shift $(\tilde{\xi}_k, \tilde{v}_k, \tilde{w}_k) \triangleq (\xi_k - \xi^*, \hat{v}_k - \hat{v}^*, w_k - w^*)$ it is straightforward to show that the error coordinates evolve with the same state-space description (7a), i.e.,

$$\tilde{v} = \left(\underbrace{\begin{bmatrix} \hat{A} & \hat{B} \\ \hat{C} & \hat{D} \end{bmatrix}}_{=: G} \otimes I_p \right) \tilde{w}. \quad (8)$$

Note that $\tilde{v}_k = \hat{v}_k - \hat{v}^* = v_k - v^*$ (eliminating the constant offset), so that by Proposition 1 the gradient and

subgradient components of (\tilde{v}, \tilde{w}) satisfy a ρ -OZF IQC. With a suitable permutation and stacking of the filters Ψ_1, Ψ_2 , we can form a compact filter Ψ such that

$$\psi_k \triangleq \begin{bmatrix} \psi_{1,k} \\ \psi_{2,k} \end{bmatrix} = (\Psi \otimes I_p) \begin{bmatrix} \tilde{v}_k \\ \tilde{w}_k \end{bmatrix}, \quad (9)$$

with $\psi_{1,k}, \psi_{2,k}$ as in Proposition 1 (with $a \triangleq v_1, b \triangleq v_2$). Define the augmented plant as the mapping $\tilde{w} \mapsto \psi$, realized as

$$\Psi \cdot \begin{bmatrix} G \\ I_2 \end{bmatrix} \triangleq \begin{bmatrix} \mathbf{A} & \mathbf{B} \\ \mathbf{C} & \mathbf{D} \end{bmatrix}. \quad (10)$$

Then the following convergence theorem holds.

Theorem 2. Take $\rho \in (0, 1)$, and filters Ψ_1, Ψ_2 that satisfy Proposition 1 with $m = \hat{m}, L = \hat{L}$. Form the augmented plant (10). If there exist $P \succ 0$ and filter coefficients of Ψ_1, Ψ_2 such that the matrix inequality

$$\begin{bmatrix} \mathbf{A}^\top P \mathbf{A} - \rho^2 P & \mathbf{A}^\top P \mathbf{B} \\ \mathbf{B}^\top P \mathbf{A} & \mathbf{B}^\top P \mathbf{B} \end{bmatrix} + \begin{bmatrix} \mathbf{C}^\top \\ \mathbf{D}^\top \end{bmatrix} \begin{bmatrix} M & 0 \\ 0 & M \end{bmatrix} [\mathbf{C} \ \mathbf{D}] \preceq 0 \quad (11)$$

holds, then (7) is exponentially stable with rate ρ , i.e.,

$$\|\xi_k - \xi^*\| \leq \sqrt{\kappa_P} \rho^k \|\xi_0 - \xi^*\|. \quad (12)$$

The proof comes as a straightforward extension of (Lessard et al., 2016, Theorem. 4) to the two-operator case, which particularly exploits the positivity constraint (6). Eq. (11) is independent of the problem dimension p , and can be used to determine the minimum worst-case convergence rate ρ via bisection. Note that Theorem 2 recovers (Nishihara et al., 2015, Theorem. 6) for $n_{\text{OZF}} = 0$.

3. A-ADMM AS A DYNAMICAL SYSTEM

Building on the previous derivations, we now formulate the A-ADMM (2)-(3) as a Lur'e system (7). In line with Nishihara et al. (2015), we introduce the coordinate change $r_k = Ax_k, s_k = Bz_k$. Moreover, define

$$\hat{f} = f \circ A^{-1}, \quad \hat{g} = g \circ B^\dagger + \mathcal{I}_{\text{im } B}, \quad (13)$$

where B^\dagger is a left-inverse of B and $\mathcal{I}_{\text{im } B}$ is the indicator of the image of B . It is straightforward to verify that $\hat{g} \in S_p(0, \infty)$ and $\hat{f} \in S_p(\hat{m}, \hat{L})$ with

$$\hat{m} = \frac{m}{\sigma^2(A)}, \quad \hat{L} = \frac{L}{\sigma^2(A)}. \quad (14)$$

Accordingly, we define the condition number of the problem as $\kappa = \frac{\hat{L}}{\hat{m}} = \kappa_f \kappa_A^2$.

Consequently, the updates (2a), (2b), (3a) can be rewritten as

$$x_{k+1} = A^{-1} \arg \min_r \hat{f}(r) + \frac{1}{2\nu_1} \|r + \hat{s}_k - c + \hat{\lambda}_k\|^2 \quad (15a)$$

$$z_{k+1} = B^\dagger \arg \min_s \hat{g}(s) + \frac{1}{2\nu_1} \|\alpha r_{k+1} - \quad (15b)$$

$$(1 - \alpha)\hat{s}_k + s - \alpha c + \hat{\lambda}_k\|^2 \quad (15c)$$

$$\hat{s}_k = s_k + \nu_2(s_k - s_{k-1}).$$

Using the definition of the proximal operator

$$\text{prox}_f(z) := \arg \min_x f(x) + \frac{1}{2} \|x - z\|^2,$$

we can summarize the A-ADMM in transformed coordinates compactly as

$$r_{k+1} = \text{prox}_{\nu_1 \hat{f}}(c - \hat{s}_k - \hat{\lambda}_k) \quad (16a)$$

$$s_{k+1} = \text{prox}_{\nu_1 \hat{g}}(\alpha c - \alpha r_{k+1} - (\alpha - 1)\hat{s}_k - \hat{\lambda}_k) \quad (16b)$$

$$\lambda_{k+1} = \alpha r_{k+1} + (\alpha - 1)\hat{s}_k + s_{k+1} - \alpha c + \hat{\lambda}_k, \quad (16c)$$

with $\hat{s}_k, \hat{\lambda}_k$ as in (15c), (3b). Next, we bring the recursion (16) into the form (7).

Proposition 3. Define the state $\xi_k \triangleq [\lambda_{k-1}^\top \ s_{k-1}^\top \ \lambda_k^\top \ s_k^\top]^\top$, output $v_k \triangleq [r_{k+1}^\top \ s_{k+1}^\top]^\top$, offset $\bar{v} \triangleq [-c^\top \ 0]^\top$, and input $w_k \triangleq [\nabla \hat{f}(r_{k+1})^\top \ \gamma_k^\top]^\top$ for any $\gamma_k \in \partial \hat{g}(s_{k+1})$. Then the sequences ξ_k , w_k , and $\hat{v}_k = v_k + \bar{v}$ satisfy (7) with the matrices

$$\begin{aligned}\hat{A} &= \begin{pmatrix} 0 & 0 & 1 & 0 \\ 0 & 0 & 0 & 1 \\ 0 & 0 & 0 & 0 \\ -\nu_2(\alpha-1) & -\nu_2 & (\alpha-1)(1+\nu_2) & 1+\nu_2 \end{pmatrix}, \\ \hat{C} &= \begin{pmatrix} \nu_2 & \nu_2 & -(1+\nu_2) & -(1+\nu_2) \\ -\nu_2(\alpha-1) & -\nu_2 & (\alpha-1)(1+\nu_2) & 1+\nu_2 \end{pmatrix}, \\ \hat{B} &= \begin{pmatrix} 0 & 0 \\ 0 & 0 \\ 0 & -\nu_1 \\ \alpha\nu_1 & -\nu_1 \end{pmatrix}, \quad \hat{D} = \begin{pmatrix} -\nu_1 & 0 \\ \alpha\nu_1 & -\nu_1 \end{pmatrix}.\end{aligned}\tag{17}$$

Proof. Apply the first-order optimality condition to the r_{k+1} and s_{k+1} updates (16a)-(16b)

$$0 = \nu_1 \nabla \hat{f}(r_{k+1}) + r_{k+1} - c + \hat{s}_k + \hat{\lambda}_k, \tag{18a}$$

$$0 \in \nu_1 \partial \hat{g}(s_{k+1}) + s_{k+1} - \alpha c + \alpha r_{k+1} + (\alpha-1)\hat{s}_k + \hat{\lambda}_k. \tag{18b}$$

Take some $\gamma_k \in \partial g(s_{k+1})$, solve for r_{k+1} and s_{k+1} , and plug it into the dual update λ_{k+1} , to get

$$r_{k+1} = -\hat{s}_k - \hat{\lambda}_k + c - \nu_1 \nabla \hat{f}(r_{k+1}), \tag{19a}$$

$$s_{k+1} = \hat{s}_k + (\alpha-1)\hat{\lambda}_k + \alpha \nu_1 \nabla \hat{f}(r_{k+1}) - \nu_1 \gamma_k, \tag{19b}$$

$$\lambda_{k+1} = -\nu_1 \gamma_k. \tag{19c}$$

Now plug in the definitions of $\hat{s}_k, \hat{\lambda}_k$ and observe that s_{k+1}, λ_{k+1} and $r_{k+1} - c$ can all be written as linear combinations of the state ξ_k and input w_k . It is then straightforward to bring ξ_{k+1} and \hat{v}_k into the matrix form (7). \square

Remark 4. In contrast to Nishihara et al. (2015), we deliberately retain the ADMM step-size ν_1 in the state-space description, instead of putting it in the sector bounds. The momentum parameter ν_2 becomes an additional degree-of-freedom.

4. PARAMETER SELECTION AND ADDITIONAL MODIFICATIONS

In unconstrained first-order methods, accelerated algorithms are parametrized by a step-size, a damping-parameter, and an extrapolation-parameter, where each quantity has provable optimal tunings (Van Scy et al., 2018). For ADMM in contrast, convergence proofs and parameter selection of ν_1, ν_2, α have been traditionally difficult. In this section we explore different parameter selection heuristics and show the influence on the convergence rates ρ that are obtained from Theorem 2. As initial heuristics, we adopt the same parameter tuning schemes of accelerated gradient methods. Next, we perform a grid-search to identify potentially superior configurations.

Table 2. Parameter selection for A-ADMM as a function of \hat{m}, \hat{L} , with $\rho := 1 - 1/\sqrt{\kappa}$.

Method	ν_1	ν_2
NM	$\frac{1}{\hat{L}}$	$\frac{\sqrt{\hat{L}} - \sqrt{\hat{m}}}{\sqrt{\hat{L}} + \sqrt{\hat{m}}}$
TM	$\frac{1+\rho}{\hat{L}}$	$\frac{\rho^2}{2-\rho}$

4.1 Nesterov and Triple Momentum Parameters

As heuristics, we use here the step-size and damping parametrization of the Nesterov method (NM) (Nesterov, 2004) and the Triple Momentum algorithm (TM) (Van Scy et al., 2018), which is known to attain the fastest possible convergence rate for accelerated gradient methods. The parameter selections are summarized in Table 2. We plot the resulting ρ obtained by Theorem 2 as a function of the condition number $\kappa = \hat{L}/\hat{m}$. We increase the O’Shea-Zames-Falb order until ρ does not improve anymore, giving $n_{OZF} = 6$ in all experiments². Fig. 1 summarizes the results for both settings, in comparison to the rates obtained from vanilla ADMM. We note that the rates of vanilla ADMM have been shown to be tight (Nishihara et al., 2015), while the curves are upper bounds.

For the NM parameter set, observe in Fig. 1a that the convergence rates substantially outperform vanilla ADMM, certifying better linear convergence across all condition numbers. Moreover, we observe that the rates asymptotically approach the optimal rate of Nesterov’s accelerated method, given by $\rho = \sqrt{1 - \frac{\sqrt{2\kappa-1}}{\kappa}}$ (Safavi et al., 2018). For the TM parameter set, observe in Fig. 1b that the convergence rates outperform vanilla ADMM in low condition regions, but from $\kappa \approx 18$ onwards, the rates degrade and eventually become infeasible. Thus, no statement about the convergence for higher condition ratios can be done. We now propose a modification to the ADMM update to alleviate this issue.

4.2 λ -Damping

Observe in (19c) that, unlike the s_k -dynamics, the λ_k dynamics depends solely on the subdifferential of \hat{g} and is therefore undamped. We propose to introduce an additional damping of the dual variable λ_k as

$$\lambda_{k+1} = d\lambda_k - d\nu_1 \gamma_k,$$

with some damping parameter $d \in (0, 1)$. From the point of view of the original algorithm iterations we can interpret this modifications by replacing the dual update in (2) with

$$\lambda_{k+1} = d(\alpha A x_{k+1} - (1-\alpha)B z_k + B z_{k+1} - \alpha c + \hat{\lambda}_k + \lambda_k). \tag{20}$$

The state-space representation of Proposition 3 is modified accordingly, with the only change occurring in the \hat{A} and \hat{B} matrix. We note that the fixed-point of the λ -damped scheme still satisfies the optimality conditions of (1), as the damping vanishes at optimality.

The results of A-ADMM with TM parameters and additional λ -damping with $d = 0.1$ are shown in Fig. 1b. We observe that convergence can now be guaranteed for all

² Code for all experiments can be found on <https://github.com/coltasas/2025-accelerated-admm>

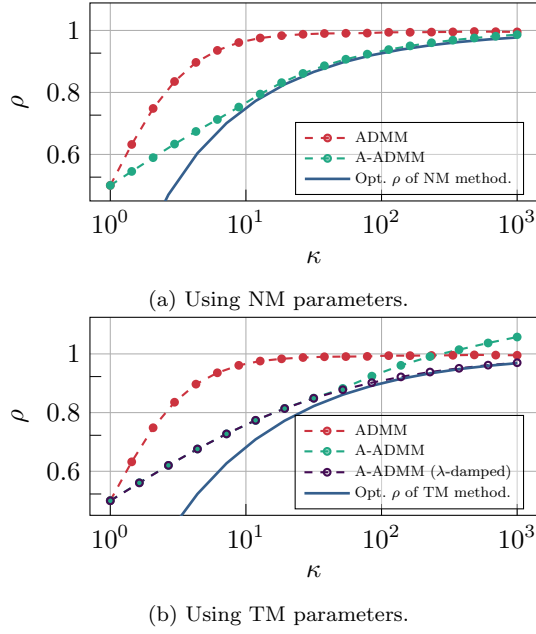


Fig. 1. Comparison of optimal ρ values for NM and TM parameterizations.

condition ratios, and as well that the rates are better than for vanilla ADMM. Moreover, we observe analogous to the NM case that the convergence rate curve approaches the optimal rate of Triple Momentum, given by $\rho = 1 - \frac{1}{\sqrt{\kappa}}$. This suggests that the additional damping of the dual variable extends the range of provable convergence for TM A-ADMM.

4.3 Grid Search Results

In addition to the already promising TM and NM parameter selections, we perform a grid search to identify potentially improved configurations of (ν_1, ν_2) . Our search is set up as a 20×20 grid centered around the TM parameters. As commonly done in strongly-convex and smooth optimization problems, we parametrize the parameters as a function of the condition ratio κ . For each κ we select (ν_1, ν_2) as the pair for which the minimal ρ can be obtained with Theorem 2 via bisection. The procedure is repeated for the over-relaxed A-ADMM (OR-A-ADMM), with an additional grid over the relaxation parameter α in the range $(0, 4]$. Note that even though the standard theory would prevent from exploring the range $(2, 4)$, we can still perform this interval extension and check for linear convergence by the feasibility of (11). Fig. 2 shows the grid search results for ν_1 and ν_2 . We found that the step-size parameter ν_1 found via grid search exactly coincides with the TM value. In contrast, the step-size parameter ν_2 exhibits a different behavior. The same holds for the over-relaxed case. Applying symbolic regression (Cranmer, 2023) reveals that ν_2 can be approximated by

$$\nu_2 \approx \left(\frac{\kappa + 0.08}{\kappa + 49.9} \right)^{\frac{1}{4}} - 0.2 \quad (21)$$

$$\nu_2^{\text{OR}} \approx \left(\frac{0.66}{\kappa + 11.97} \right) \kappa + 0.06, \quad (22)$$

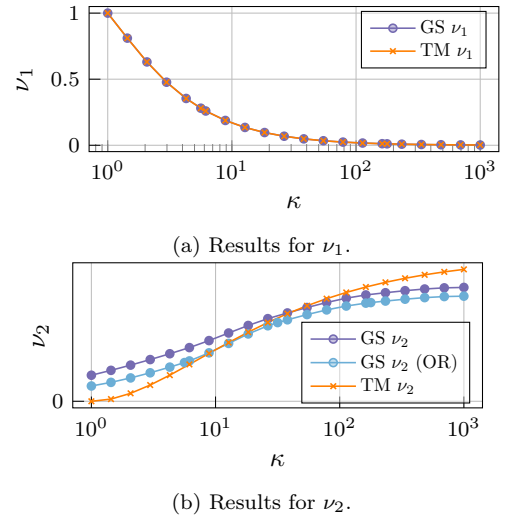


Fig. 2. Results of the grid search for (ν_1, ν_2) vs. TM parameters from Table 2.

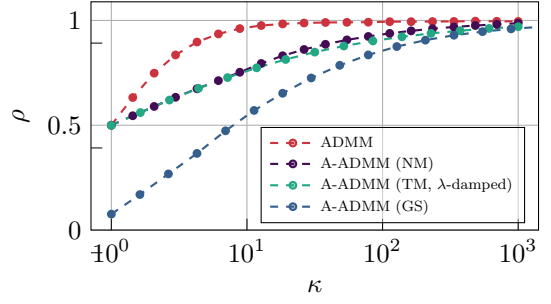


Fig. 3. Comparison of optimal ρ values for ADMM and A-ADMM with different parameter configurations.

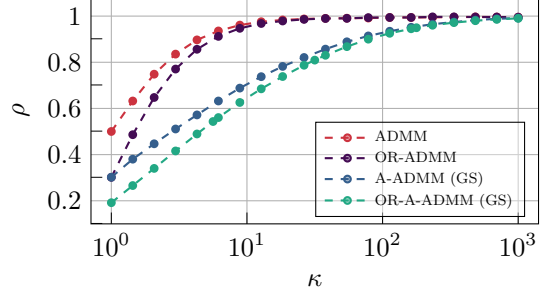


Fig. 4. Comparison of optimal ρ values nominal and over-relaxed ADMM versions.

for the nominal and over-relaxed settings, respectively. The over-relaxation parameter α was found to be optimal for $\alpha \approx 1.45$ across all condition numbers.

Fig. 3 summarizes the convergence rates obtained from the grid search (GS) parameters, in comparison to the vanilla ADMM method and the accelerated versions with NM and TM parameters. By design, the A-ADMM with GS-parameters gives the best linear convergence rate of A-ADMM among all settings. Fig. 4 complements the results with the over-relaxed variants. We observe that the over-relaxed variants constantly outperform the non-over-relaxed ones; and that the accelerated variants constantly outperform the non-accelerated variants. Moreover, A-ADMM also outperforms the vanilla over-relaxed ADMM.

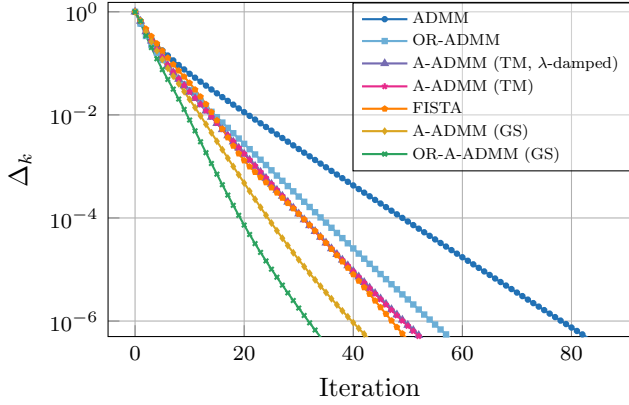


Fig. 5. Empirical performance of different A-ADMM schemes and other benchmark algorithms applied to LASSO regression.

5. CASE STUDY

We test the A-ADMM schemes designed based on the theoretical analyses in the previous section on the ℓ_1 -regularized least-squares problem, also known as LASSO Regression, and compare them with available algorithms (Boyd et al., 2011). We use the benchmark problem

$$\begin{aligned} \min_{x,z} \quad & \frac{1}{2} \|Fx - b\|_2^2 + \tau \|z\|_1 \\ \text{s.t.} \quad & x = z, \end{aligned} \quad (23)$$

where $F \in \mathbb{R}^{250 \times 100}$ is chosen as a tall and full column rank matrix with entries that are sampled i.i.d. from an isotropic Gaussian distribution $\mathcal{N}(0, 1)$, with normalized columns. The vector b is generated as $b = Fw^0 + \varepsilon$, where $w^0 \in \mathbb{R}^{100}$ is sparse, containing 50 non-zeros drawn from $\mathcal{N}(0, 1)$ and $\varepsilon \sim \mathcal{N}(0, 10^{-3}I_{250})$. The regularization parameter $\tau > 0$, is set to $\tau = 0.01$. Problem (23) fits the general problem (1), where the first term is m -strongly convex and L -smooth with $m = \underline{\sigma}^2(F^\top F)$ and $L = \bar{\sigma}^2(F^\top F)$.

Applying the accelerated over-relaxed ADMM results in

$$x_{k+1} = (\nu_1 F^\top F + I)^{-1} \left(-\hat{z}_k - \hat{\lambda}_k + \nu_1 F^\top b \right), \quad (24a)$$

$$z_{k+1} = \mathcal{S}_{\tau\nu_1} \left(-\alpha x_{k+1} - (\alpha - 1)\hat{z}_k - \hat{\lambda}_k \right), \quad (24b)$$

$$\lambda_{k+1} = \alpha x_{k+1} + (1 - \alpha) \hat{z}_k + z_{k+1} + \hat{\lambda}_k, \quad (24c)$$

$$\hat{z}_k = z_k + \nu_2 (z_k - z_{k-1}), \quad (24d)$$

$$\hat{\lambda}_k = \lambda_k + \nu_2 (\lambda_k - \lambda_{k-1}). \quad (24e)$$

with the soft-thresholding operator $\mathcal{S}_{\tau\nu_1}$ that is (element-wise) defined as

$$[\mathcal{S}_{\tau\nu_1}(\mathbf{y})]_i = \text{sign}(\mathbf{y}_i) \max(|\mathbf{y}_i| - \tau\nu_1, 0). \quad (25)$$

The convergence is assessed through the normalized iterate error

$$\Delta_k := \frac{\|x_k - x^*\|_2}{\|x_0 - x^*\|_2}, \quad (26)$$

where x^* is the solution of (23).

In particular, we study the convergence speed of A-ADMM and OR-A-ADMM, both with TM and GS parameters, against the widely used LASSO benchmark solver FISTA (Beck and Teboulle, 2009) as well as ADMM and OR-ADMM.

As shown in Figure 5, the A-ADMM methods with proposed tunings consistently achieve faster convergence compared to both the vanilla ADMM and existing accelerated algorithms from the literature. Within our family of methods, the OR-variant provides a clear advantage as it always outperforms the nominal counterparts. The grid search parameter set yields the best result. We also observe that the TM version with and without λ -damping show almost identical empirical performance. Notably, the ordering of algorithms evaluated on the empirical performance and evaluated on the worst-case convergence rates stays the same, suggesting that the worst-case convergence rate is a suitable metric for algorithm comparison.

6. CONCLUSIONS

This paper used the IQC-based algorithm analysis framework to show linear convergence rates of different accelerated ADMM variants. We proposed different parameter tunings and show that all variants outperform vanilla ADMM. The fastest version both in terms of certified convergence rate and empirical performance was found using a grid search over the parameter space, giving the fastest version of A-ADMM in the strongly-convex-smooth setting to date. We moreover showed the close connection between A-ADMM parameters and accelerated gradient methods from unconstrained optimization. Future works could focus on theoretic derivations of the optimal A-ADMM parameters with tools from systems theory, and the development of a systematic and robust A-ADMM synthesis procedure.

REFERENCES

Beck, A. and Teboulle, M. (2009). A fast iterative shrinkage-thresholding algorithm for linear inverse problems. *SIAM Journal on Imaging Sciences*.

Boczar, R., Lessard, L., and Recht, B. (2015). Exponential convergence bounds using integral quadratic constraints. In *2015 54th IEEE Conference on Decision and Control (CDC)*.

Boyd, S., Parikh, N., Chu, E., Peleato, B., and Eckstein, J. (2011). Distributed optimization and statistical learning via the alternating direction method of multipliers. *Foundations and Trends in Machine Learning*.

Cranmer, M. (2023). Interpretable machine learning for science with PySR and SymbolicRegression.jl. arXiv:2305.01582.

Deng, W. and Yin, W. (2016). On the global and linear convergence of the generalized alternating direction method of multipliers. *Journal of Scientific Computing*.

Eckstein, J. and Bertsekas, D.P. (1992). On the Douglas—Rachford splitting method and the proximal point algorithm for maximal monotone operators. *Mathematical Programming*.

Glowinski, R. and Marroco, A. (1975). Sur l'approximation, par éléments finis d'ordre un, et la résolution, par pénalisation-dualité d'une classe de problèmes de dirichlet non linéaires. *ESAIM: Mathematical Modelling and Numerical Analysis—Modélisation Mathématique et Analyse Numérique*.

Goldstein, T., O'Donoghue, B., Setzer, S., and Baraniuk, R. (2014). Fast alternating direction optimization methods. *SIAM Journal on Imaging Sciences*.

Lessard, L., Recht, B., and Packard, A. (2016). Analysis and design of optimization algorithms via integral quadratic constraints. *SIAM Journal on Optimization*.

Megretski, A. and Rantzer, A. (1997). System analysis via integral quadratic constraints. *IEEE Transactions on Automatic Control*.

Michalowsky, S., Scherer, C., and Ebenbauer, C. (2021). Robust and structure exploiting optimisation algorithms: an integral quadratic constraint approach. *International Journal of Control*, 94(11), 2956–2979.

Nesterov, Y. (2004). *Introductory lectures on convex optimization*. Springer Science & Business Media.

Nishihara, R., Lessard, L., Recht, B., Packard, A., and Jordan, M. (2015). A general analysis of the convergence of ADMM. In *Proceedings of the 32nd International Conference on Machine Learning*.

Notarstefano, G., Notarnicola, I., and Camisa, A. (2019). Distributed optimization for smart cyber-physical networks. *Foundations and Trends in Systems and Control*.

Patrinos, P., Stella, L., and Bemporad, A. (2014). Douglas-Rachford splitting: Complexity estimates and accelerated variants. In *53rd IEEE Conference on Decision and Control*.

Pejcic, I. and Jones, C.N. (2016). Accelerated ADMM based on accelerated Douglas-Rachford splitting. *Proc. European Control Conference (ECC)*.

Safavi, S., Joshi, B., França, G., and Bento, J. (2018). An explicit convergence rate for Nesterov's method from SDP. In *2018 IEEE International Symposium on Information Theory (ISIT)*, 1560–1564. IEEE.

Upadhyaya, M., Banert, S., Taylor, A.B., and Giselsson, P. (2024). Automated tight Lyapunov analysis for first-order methods. *Mathematical Programming*.

Van Scy, B., Freeman, R.A., and Lynch, K.M. (2018). The fastest known globally convergent first-order method for minimizing strongly convex functions. *IEEE Control Systems Letters*.

Wang, D., He, Y., and Sterck, H.D. (2021). On the asymptotic linear convergence speed of Anderson acceleration applied to ADMM. *Journal of Scientific Computing*.